World Landslide Forum

Sentinel-1 data analysis for landslide detection and mapping: first experiences in Italy and Spain

--Manuscript Draft--

Manuscript Number:	WLFO-D-16-00483R4
Full Title:	Sentinel-1 data analysis for landslide detection and mapping: first experiences in Italy and Spain
Article Type:	***Vol. 3 – Advances in Landslide Technology***
Section/Category:	Vol. 3 - Session 1 - Landslide Monitoring and Warning
Funding Information:	
Abstract:	One of the key inputs to landslide susceptibility and hazard analyses is provided by a precise inventory map, including the information of landslide activity. In the last decade the satellite SAR Interferometry has been demonstrated to be a powerful tool for landslide mapping and monitoring. However, until now, the systematic use of the technique has been strongly limited by different aspects like the image availability, the revisit time and the loss of coherence. In this context, the Sentinel-1 constellation provides interesting characteristics for landslide mapping and monitoring: the wavelength (55.5 mm) and the short temporal baseline (6 days when Sentiel-1B data will be available). The latter one is expected to be a key feature for increasing coherence and for defining monitoring and updating plans. However, the exploitation of these high coherent data for landslide purposes is not straightforward and demands of new tools and methods to properly discriminate the real displacements. The aim of this work is to show which are, according to the authors experience, the main pros and cons of landslides mapping and monitoring with Sentinel-1 data. These conclusions are based on the analysis over three different test sites with different characteristics from the SAR view point: the Canarias Islands (Spain), the Molise region (Italy) and the Toscana region (Italy). The Canarias Islands test site shows a good example of how Sentinel-1 can systematically provide deformation maps over wide areas and with a very high sampling density. The Molise region application shows how the short temporal revisit time of Sentinel-1 allows the detection and monitoring of landslides also over agricultural areas. In particular, for this test site, are shown some examples of detection and update of active landslide phenomena. Finally, in the third example, the Toscana area, we show another example of difficult scenario, where the high temporal sampling has allowed the detection of some landslide phenomena. However, this test site is also a good example to show one of the main problems to be solved when applying short temporal baseline interferometry in rural environments: false deformation trends related to soil changes.
Corresponding Author:	Anna Barra CTTC SPAIN
Corresponding Author Secondary Information:	
Corresponding Author's Institution:	CTTC
Corresponding Author's Secondary Institution:	
First Author:	Anna Barra
First Author Secondary Information:	
Order of Authors:	Anna Barra
	Oriol Monserrat
	Nuria Devanthery
	Maria Cuevas-Gonzalez
	Guido Luzi
	Michele Crosetto

	Bruno Crippa
Order of Authors Secondary Information:	
Author Comments:	
Response to Reviewers:	Dear Editor, Thank you for your comments. Now the manuscript should be consistent with the template and I hope the Figures are more clear. Best regards, Anna Barra

Sentinel-1 data analysis for landslide detection and mapping: first experiences in Italy and Spain

Anna Barra, Oriol Monserrat, Michele Crosetto, María Cuevas-Gonzalez, Núria Devanthéry, Guido Luzi, Bruno Crippa

Abstract

The differential interferometric SAR (DInSAR) technique is a powerful tool to detect and monitor ground deformation. In this paper we address an important DInSAR application, which is the detection and mapping of landslides. The potential of DInSAR to detect and monitor landslides has been extensively documented in the literature, mainly using the C-band data from the European Remote Sensing (ERS-1 and -2), Envisat and Radarsat missions. A significant improvement in landslide monitoring is expected by the SAR data of the two satellites Sentinel-1A and -1B of the European Space Agency. This paper describes the authors' first experience using Sentinel-1 for landslide monitoring. The paper describes the data processing and analysis strategy, and then illustrates some deformation measurement results obtained over Italy and Spain.

Keywords

SAR, interferometry, Sentinel-1, landslide, detection, mapping, monitoring.

Introduction

This paper is focused on the detection and mapping of landslides using the differential interferometric SAR (DInSAR) technique with Sentinel-1 satellite images. DInSAR is a powerful tool to detect and monitor ground deformation. It has been widely exploited in almost the last three decades, yielding significant results in several fields, like seismology (Massonnet et al, 1993; Dalla Via et al, 2012), vulcanology (Massonnet et al, 1995; Antonielli et al. 2014), landslides (Carnec et al, 1996; García-Davalillo et al, 2014), glaciology (Goldstein et al, 1993), ground subsidence and uplift (Galloway et al, 1998), etc. A review of different DInSAR applications is provided by Massonnet and Feigl (1998).

An advanced class of the DInSAR techniques is given by Persistent Scatterer Interferometry (PSI), see for a review Crosetto et al. (2016). The PSI techniques require large stacks of SAR images acquired over the same area. Through appropriate data processing and analysis procedures, they yield better deformation monitoring results, when compared with the DInSAR results, both in terms of precision and reliability. This paper describes a simplified PSI procedure to perform landslide detection and monitoring using SAR data acquired by the Sentinel-1 satellite of the European Space Agency.

As mentioned above, DInSAR has been used since almost three decades; it was introduced the first time by Gabriel et al. (1989). Since then, several satellite mission have been performed that have provided very reach archives of SAR data. Starting at the beginning of 90s, the most important SAR data sources have been three missions: the two European Remote Sensing (ERS) satellites, ERS-1 and –2; the Envisat and the Radarsat missions. All of them were acquiring C-band data, with an approximate wavelength of 5.5 cm. An important characteristic of these missions is that they cover time periods of several years. In this way they allow us performing a long-term deformation monitoring. In addition, their satellites performed the so-called background missions, i.e. the systematic and regular acquisition over wide areas. This is a key feature that generated very rich SAR data archives, which allow us performing "deformation measurements back in time": this is an unmatched capability of the DInSAR and PSI techniques.

In 2007, started two new important missions: TerraSAR-X and COSMO-SkyMed. Both of them provide very high resolution SAR imagery, with pixel footprints of the order of 1 meter. They work with X-band data, with an approximate wavelength of 3 cm. These type of data provide a very dense measurement sampling, with a high sensitivity to small displacements, e.g. see Crosetto et al. (2010). The major drawbacks of these data are the on-demand data acquisition policy (this is the opposite philosophy of the above mentioned background mission policy), the relative high price of the images. These two aspects

strongly limit the applicability for landslide detection and monitoring.

A significant further mission is given by the satellites Sentinel-1A and –1B. These satellites acquire C-band data. They offer an improved data acquisition capability with respect to previous C-band sensors, increasing considerably the deformation monitoring potential. In their standard data acquisition mode (Interferometric Wide Swath - IWS), they acquire images covering 250 by 180 km with a revisiting cycle of 12 days, which becomes 6 days using both Sentinel-1 satellites. The improved Sentinel-1 coverage is essential to develop wide-area PSI monitoring applications, e.g. landslide monitoring while the shorter revisit time provides a better coherence of the interferograms.

It is worth underlining that the Sentinel-1 mission acquire data in background mode. Over several regions of the world, starting with Europe, the data acquisition is temporally very dense. However, one has to consider that the temporal sampling is rather uneven over the globe, with several regions not covered by the Sentinel-1 data. A final key advantage of Sentinel-1 data is that they are available free of charge to all data users: general public, scientific and commercial users.

This article describes the authors' first experience with Sentinel-1. The next section describes the data processing and analysis strategy. The following one illustrates some deformation measurement results obtained over Italy and Spain.

Data processing and analysis

Most of the SAR data available before the launch of Sentinel-1 were acquired using the standard StripMap acquisition mode. Sentinel-1 data use another, more sophisticated, data acquisition procedure: the TOPS (Terrain Observation by Progressive Scan) imaging mode (Yague-Martinez et al, 2016). This mode is key to achieve the wide area Sentinel-1 coverage. The drawback is that the Sentinel-1 IWS data require extra processing: in fact, the TOPS acquisition geometry, and in particular the variable squint angle, requires a more complex elaboration of the SAR images. The extra processing mainly concerns the image co-registration step, which needs to be very accurate (Prats-Iraola et al, 2012).

After the precise image co-registration, in order to process and analyse Sentinel-1 interferometric data, we use a two-stage procedure: a DInSAR analysis and a Multilayer GIS analysis.

The first stage is performed in the original SAR geometry. Starting from the stack of SAR images that cover the same area of interest, a set of interferograms is generated. The interferograms are then analysed both spatially and temporally with the aim of detecting areas affected by deformation. The main output of this step is a set of areas potentially affected by deformation.

The second stage, which is called multi-layer GIS analysis, consists in the integration of the DInSAR derived data with geological and geomorphological data in order to interpret and validate the detected areas of deformation. This information can then be used to update the pre-existing landslide inventory maps.

In the following we describe the main steps of the procedure.

- **Interferogram generation**. Starting from the stack of complex SAR images, we generate the network of interferograms to be used in the analysis. Typically, only the interferometric pairs with the minimum temporal baseline (using Sentinel-1A data, 12 days) are used.

- **Spatial analysis**. The spatial analysis consists in the visual inspection of the single interferograms in order to identify spatial patterns associated with potential deformation areas. It is worth noting that this type of analysis can only be used to detect deformation phenomena that are fast enough to be observed in 12-day periods, i.e fast enough to generate phase patterns that are visible in single interferograms.

- **Analysis of pairs of interferograms**. Once the patterns are detected, the pairwise logic approach described in Massonnet and Feigl (1995) is used. It is useful for discriminating the deformation signal from artifacts (mainly the residual topographic errors and the atmospheric effects). The output of this step is a set of areas potentially affected by deformation.

- **Temporal analysis.** This step involves the phase unwrapping of the interferograms. We use for this the Minimum Coast Flow approach. The phase unwrapping is done only for those pixels with a coherence value higher than a given threshold. Starting from the unwrapped interferograms, we derive the phase temporal series in correspondence of the image acquisition dates. This is obtained by directly integrating the unwrapped phases (Barra et al, 2016).

The above time series are then analysed to identify new spatial phase patterns characterized by slow deformation rates. It is worth noting that the analysis of the time series is done with respect to a local stable reference in order to minimize the atmospheric effects.

- **Spatio-temporal analysis**. The potential deformation areas identified in the previous steps are analyzed together with the time series. This analysis is addressed to the following aspects. Firstly, detecting the errors occurred during the phase unwrapping step. Secondly, assessing the temporal behavior of each detected deformation phenomenon. And thirdly confirming or modifying the shape of the detected

deformation areas. The result is the final set of detected deformation phenomena.

- **Geocoding**. The detected deformation area are finally transformed to an external reference system, i.e. to geographic or cartographic coordinates.

- **Multilayer GIS analysis**. The information coming from the previous step is then combined, in a GIS environment, with different information layers: a digital elevation model, aspect and slope, ortoimages geo-lithological maps, existing landslide inventory maps, etc. These layer are used to carry out a geological and geomorphological interpretation, to confirm, deny or modify the DInSAR results.

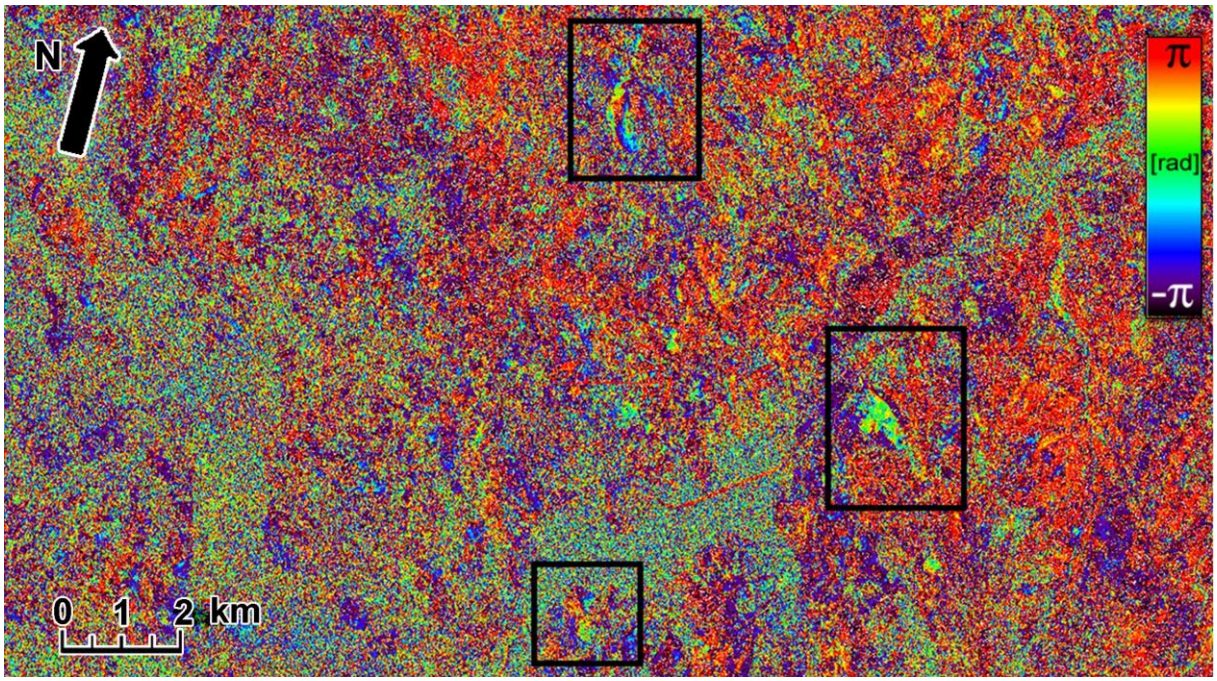

Fig. 1 Example of three potential deformation patterns identified in a 12-day wrapped interferogram.

Examples of results

The procedure described above was successfully used to study an area located in the Molise region, in Southern Italy. The study area is affected by a great number of landslide phenomena, see for details Barra et al. (2016). The analysis was based on 14 ascending images acquired in the period from October 2014 to April 2015. Figure 1 shows some examples of potential deformation patterns that were identified using a 12-day wrapped interferogram. Three main patterns are highlighted by black squares.

Figure 2 shows one of the landslides of the study area. The upper left image (a) displays a 12-day interferogram. Even over such a short time period, a landslide deformation pattern can be detected in this interferogram. The approximate border of the landslide is highlighted by a white contour superposed to the colour-coded interferometric values. The upper right figure (b) displays the accumulated deformation. In this case, the deformation pattern of the above landslide can be clearly distinguished from the surrounding areas. The observed displacement, shown in blue, is toward the satellite. The maximum line-of-sight recorded displacement of the landslide is up to 13 cm. The lower image (c) illustrates a deformation time series of the landslide. In this case, the time series shows the average displacements of the entire landslide. One may notice that a period of quiescence occurs between the third and the sixth image, which is followed by an acceleration period.

Figure 3 shows an example of outcome of the multilayer GIS analysis: a set of confirmed landslides. The landslides are superposed to the accumulated deformation map. The border of each landslide, shown in red, has been updated on the bases of the optical and morphological interpretation performed in a GIS environment. The landslides in the rectangle 2 (Figure 3) are represented in Figure 4, over an optical image, together with the Italian landslide inventory map (IFFI): the existing inventory (IFFI) has been updated in terms of spatial and temporal activity thanks to the integration of DInSAR and Multilayer GIS analysis.

Further details of this analysis are described in Barra et al. (2016).

Finally, Figure 5 shows an example of accumulated deformation map of the Tenerife Island (Canary Islands, Spain). 34 Sentinel-1 images, acquired during the period spanning from 5th November 2014 to 4th February 2016, were used. The data were processed with a multi-look of 2 by 10 (azimuth by range), which corresponds to a footprint of approximately 28 by 40 m. This resolution is a compromise between density of measureable points, which is related to coherence, and resolution, which needs to be high enough to detect small deformation phenomena.

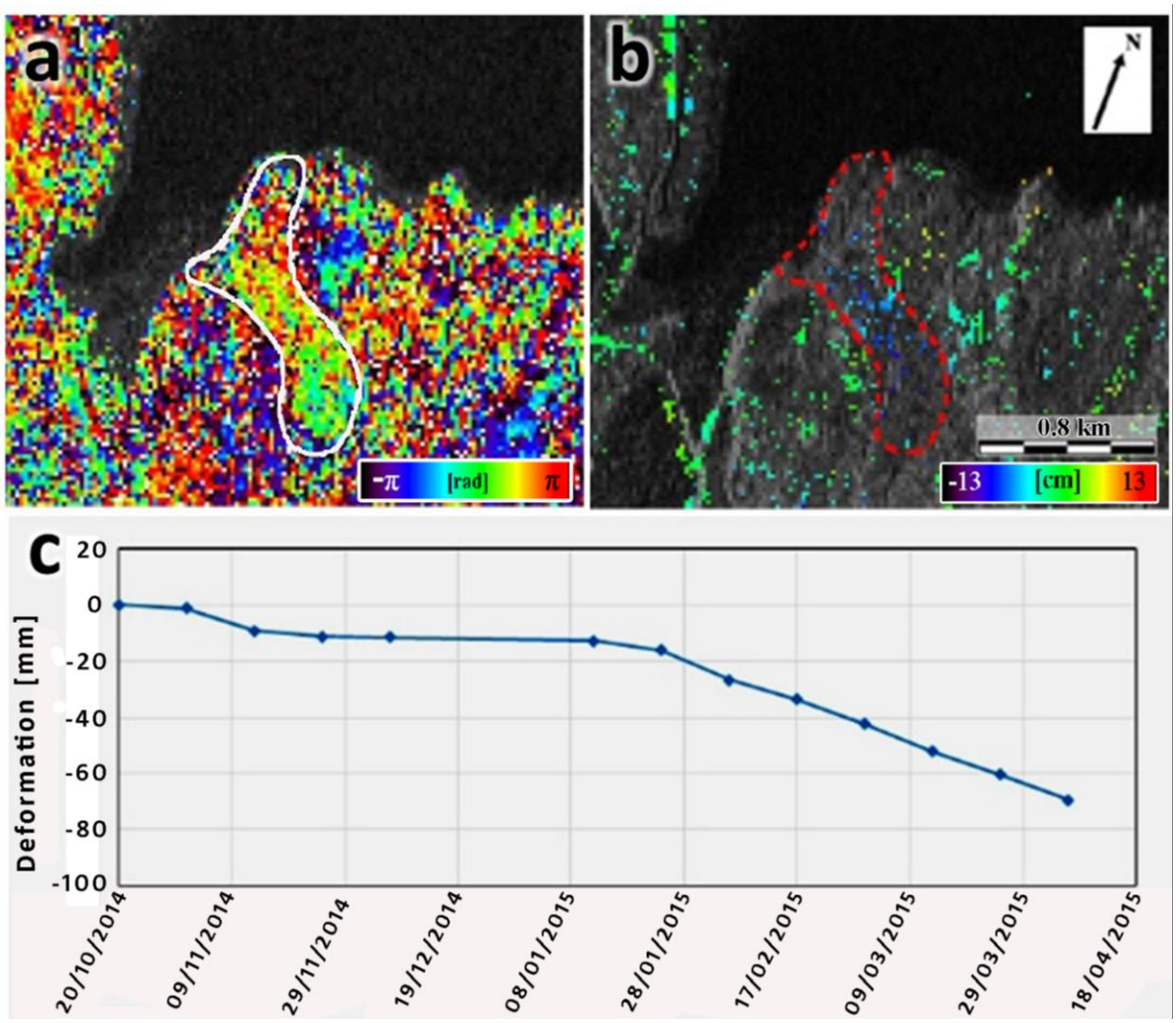

Fig. 2 Example of a detected landslide in a 12-days interferogram (a) and in the accumulated deformation map (b). The contour of the detected landslide is in white in (a) and in red in (b). In (c), the mean deformation time series of the landslide.

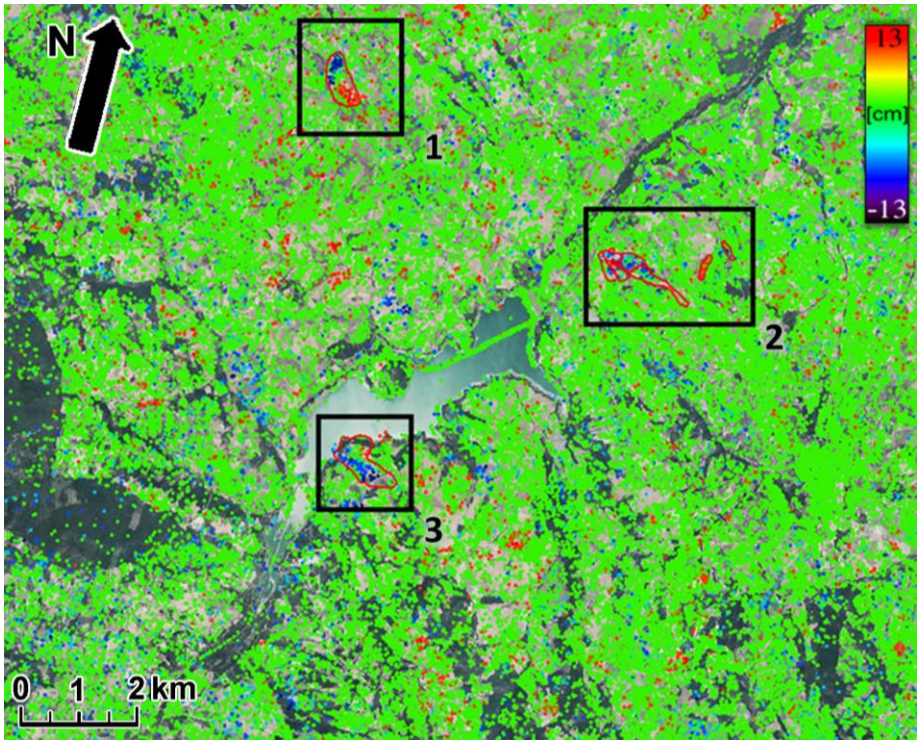

Fig. 3 Accumulated deformation map with examples of landslides confirmed in the multilayer GIS analysis, by analysing the optical images and the thopography.

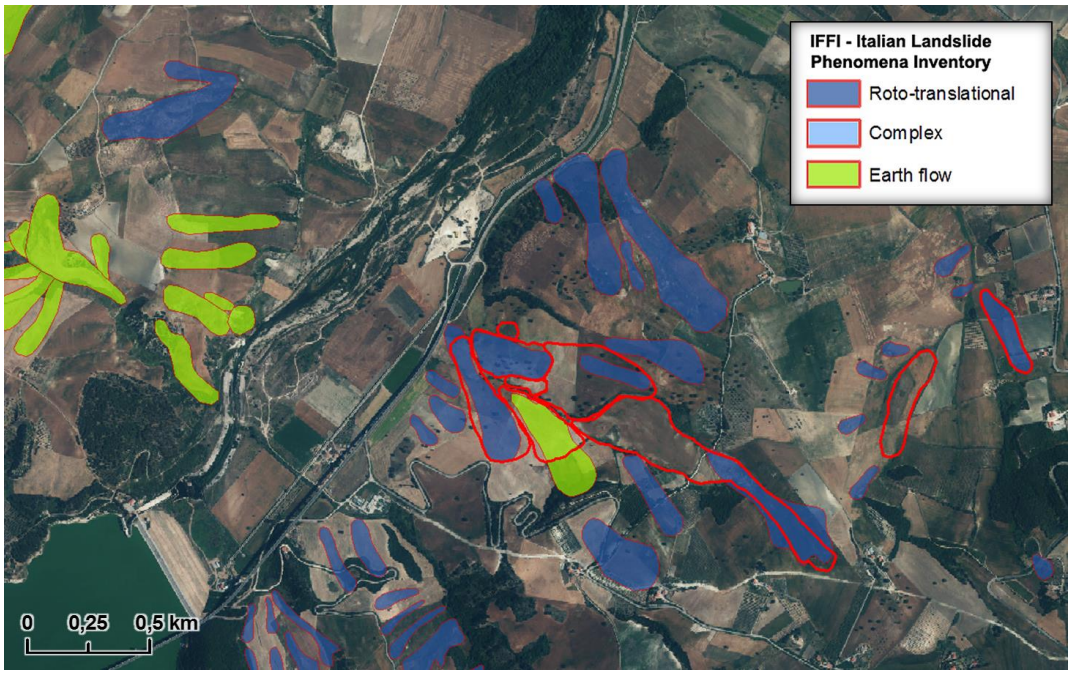

Fig. 4 In red, landslides outlined in the GIS multilayer analysis. In geen and blue, the Italian Landslide Phenomena Inventory (IFFI). The deformation areas identified in DInSAR analysis (see the accumulated deformation map in Figure 3, rectangle 2) have been confirmed to be lanslides and outlined in detail through the GIS multilayer analysis. The Italian inventory map (IFFI) has been updated in terms of spatial and temporal activity.

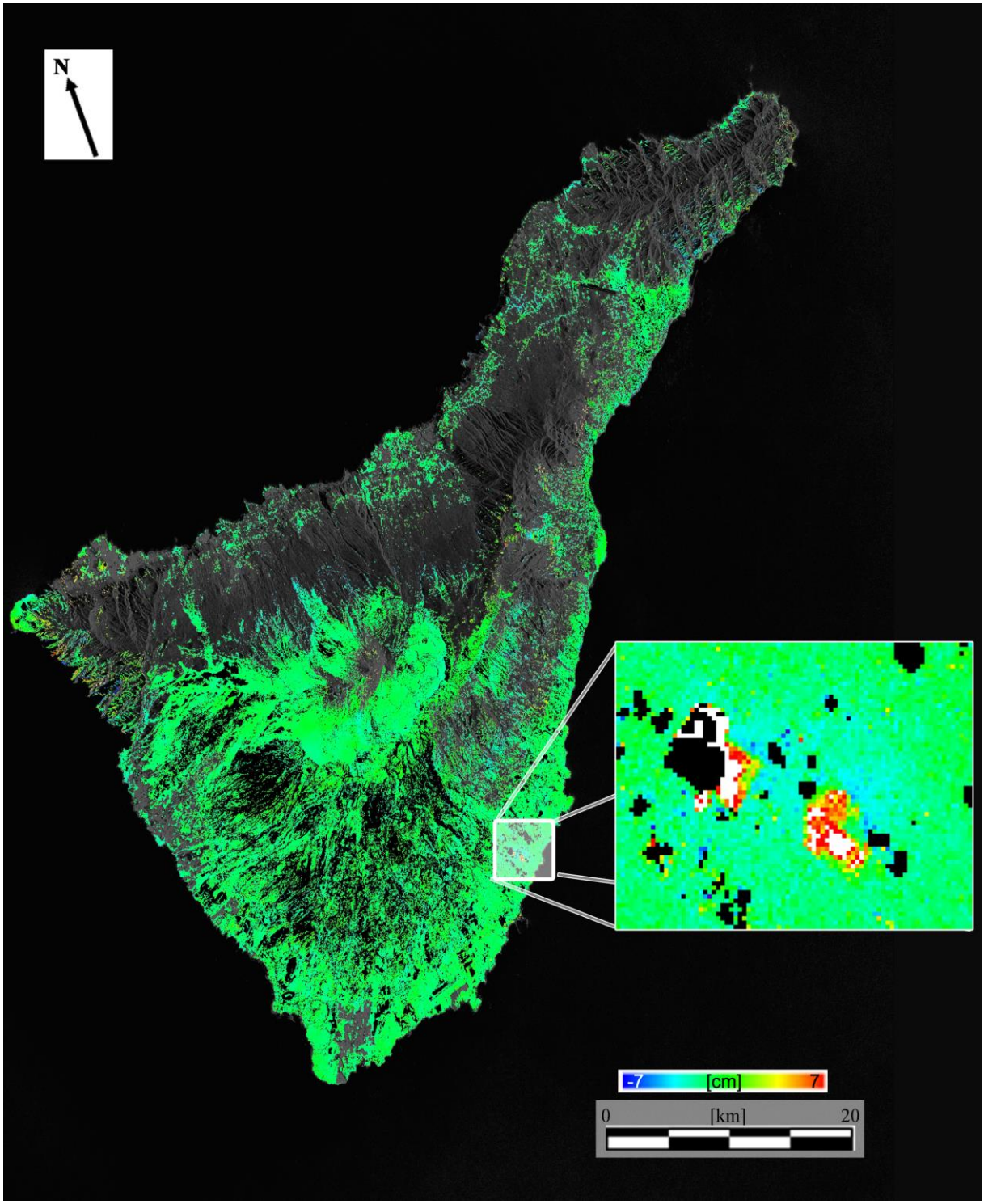

Fig. 5 Accumulated deformation map of the Tenerife Island (Canary Islands, Spain) derived using a stack of Sentinel-1 images. Zoom over a deformation associated with a landfill waste.

Acknowledgments

This work has been partially funded by the Spanish Ministry of Economy and Competitiveness through the project MIDES (Ref: CGL2013-43000-P).

References

Antonielli B, Monserrat O, Bonini M, Righini G, Sani F, Luzi G, Feyzullayev A A, Aliyev C S, (2014) Pre-eruptive ground deformation of Azerbaijan mud volcanoes detected through satellite radar interferometry (DInSAR). Tectonophysics. 637: 163-177.

Barra A, Monserrat O, Mazzanti P, Esposito C, Crosetto M, Scarascia Mugnozza G, (2016) First insights on the potential of Sentinel-1 for landslides detection. Geomatics, Natural Hazards and Risks. 7(6): 1874-1883.

Carnec C, Massonnet D, King C, (1996) Two examples of the use of SAR interferometry on displacement fields of small spatial extent. Geophysical Research Letters, 23(24): 3579-3582.

Crosetto M, Monserrat O, Cuevas-González M, Devanthéry N, (2016) Persistent Scatterer Interferometry: a review. ISPRS J. of Photogrammetry and Remote Sensing. 115: 78-89.

Crosetto M, Monserrat O, Iglesias R, Crippa B, (2010) Persistent Scatterer Interferometry: potential, limits and initial C- and X-band comparison". Photogrammetric Engineering & Remote Sensing. 76(9): 1061-1069.

Dalla Via G, Crosetto M, Crippa B, (2012) Resolving vertical and east-west horizontal motion from differential interferometric synthetic aperture radar: The L'Aquila earthquake. Journal of Geophysical Research: Solid Earth (1978–2012). 117(B2).

Gabriel A K, Goldstein R M, Zebker H A, (1989) Mapping small elevation changes over large areas: differential radar interferometry. J. Geophys Res. 94 (B7): 9183-9191.

Galloway D.L, Hudnut K W, Ingebritsen S E, Phillips S P, Peltzer G, Rogez F, Rosen P A, (1998) Detection of aquifer system compaction and land subsidence using interferometric synthetic aperture radar, Antelope Valley, Mojave Desert, California. Water Resources Research. 34(10): 2573-2585.

García-Davalillo J C, Herrera G, Notti D, Strozzi T, Álvarez-Fernández I, (2014) DInSAR analysis of ALOS PALSAR images for the assessment of very slow landslides: the Tena Valley case study. Landslides. 11(2): 225-246.

Goldstein R M, Engelhardt H, Kamb B, Frolich R M, (1993) Satellite radar interferometry for monitoring ice sheet motion: application to an Antarctic ice stream. Science. 262(5139): 1525-1530.

Massonnet D, Briole P, Arnaud A, (1995) Deflation of Mount Etna monitored by spaceborne radar interferometry. Nature. 375: 567-570.

Massonnet D, Feigl K L. (1995) Discriminating geophysical phenomena in satellite radar interferograms. Geophys. Res. Lett. 22: 1537-1540.

Massonnet D, Feigl K L, (1998) Radar interferometry and its application to changes in the Earth's surface. Reviews of geophysics. 36(4): 441-500.

Massonnet D, Rossi M, Carmona C, Adragna F, Peltzer G, Feigl K, Rabaute T, (1993) The displacement field of the Landers earthquake mapped by radar interferometry. Nature. 364(6433): 138-142.

Prats-Iraola P, Scheiber R, Marotti L, Wollstadt S, Reigber A, (2012). TOPS interferometry with TerraSAR-X. IEEE TGRS. 50(8): 3179-3188.

Yague-Martinez N, Prats-Iraola P, Rodriguez Gonzalez F, Brcic R, Shau R, Geudtner D, Eineder M, Bamler R (2016) Interferometric Processing of Sentinel-1 TOPS Data. IEEE Transactions on Geoscience and Remote Sensing. 54(4): 2220-2234.

Anna Barra (✉)
Centre Tecnològic de Telecomunicacions de Catalunya (CTTC), Division of Geomatics, Av. Gauss 7, E-08860 Castelldefels 08860, Barcelona, Spain
E-mail: abarra@cttc.cat
Oriol Monserrat
Centre Tecnològic de Telecomunicacions de Catalunya (CTTC), Division of Geomatics, Av. Gauss 7, E-08860 Castelldefels 08860, Barcelona, Spain
E-mail: omonserrat@cttc.cat
Michele Crosetto
Centre Tecnològic de Telecomunicacions de Catalunya (CTTC), Division of Geomatics, Av. Gauss 7, E-08860 Castelldefels 08860, Barcelona, Spain
E-mail: mcrosetto@cttc.cat
María Cuevas-Gonzalez
Centre Tecnològic de Telecomunicacions de Catalunya (CTTC), Division of Geomatics, Av. Gauss 7, E-08860 Castelldefels, Barcelona, Spain
E-mail: mcuevas@cttc.cat
Núria Devanthery
Centre Tecnològic de Telecomunicacions de Catalunya (CTTC), Division of Geomatics, Av. Gauss 7, E-08860 Castelldefels 08860, Barcelona, Spain
E-mail: ndevanthery@cttc.cat
Guido Luzi
Centre Tecnològic de Telecomunicacions de Catalunya (CTTC), Division of Geomatics, Av. Gauss 7, E-08860 Castelldefels 08860, Barcelona, Spain
E-mail: gluzi@cttc.cat
Bruno Crippa
Department of Earth Sciences, University of Milan, Via Cicognara 7, I-20129 Milan, Italy
E-mail: bruno.crippa@unimi.it